

## PDF hosted at the Radboud Repository of the Radboud University Nijmegen

The following full text is a publisher's version.

For additional information about this publication click this link.

<https://hdl.handle.net/2066/220073>

Please be advised that this information was generated on 2021-10-16 and may be subject to change.



# Estimating ankle torque and dynamics of the stabilizing mechanism: No need for horizontal ground reaction forces



I.M. Schut<sup>a,\*</sup>, J.H. Pasma<sup>a,b</sup>, J.M.B. Roelofs<sup>c</sup>, V. Weerdesteyn<sup>c,d</sup>, H. van der Kooij<sup>a,e</sup>, A.C. Schouten<sup>a,e</sup>

<sup>a</sup> Biomechanical Engineering Department at the Delft University of Technology, Delft 2628 CD, Netherlands

<sup>b</sup> Department of Orthopaedic Surgery at the Haga Hospital, The Hague 2545 AA, Netherlands

<sup>c</sup> Department of Rehabilitation, Donders Centre for Neuroscience, Radboud University Medical Center, Nijmegen, Netherlands

<sup>d</sup> Sint Maartenskliniek Research, Development and Education, Nijmegen, Netherlands

<sup>e</sup> Biomechanical Engineering Department at the University of Twente, Enschede 7522 LW, Netherlands

## ARTICLE INFO

### Article history:

Accepted 20 April 2020

### Keywords:

Ankle torque  
Stiffness  
Stabilizing mechanism  
System identification  
Treadmill

## ABSTRACT

Changes in human balance control can objectively be assessed using system identification techniques in combination with support surface translations. However, large, expensive and complex motion platforms are required, which are not suitable for the clinic. A treadmill could be a simple alternative to apply support surface translations. In this paper we first validated the estimation of the joint stiffness of an inverted pendulum using system identification methods in combination with support surface translations, by comparison with the joint stiffness calculated using a linear regression method. Second, we used the system identification method to investigate the effect of horizontal ground reaction forces on the estimation of the ankle torque and the dynamics of the stabilizing mechanism of 12 healthy participants. Ankle torque and resulting frequency response functions, which describes the dynamics of the stabilizing mechanism, were calculated by both including and excluding horizontal ground reaction forces. Results showed that the joint stiffness of an inverted pendulum estimated using system identification is comparable to the joint stiffness estimated by a regression method. Secondly, within the induced body sway angles, the ankle torque and frequency response function of the joint dynamics calculated by both including and excluding horizontal ground reaction forces are similar. Therefore, the horizontal ground reaction forces play a minor role in calculating the ankle torque and frequency response function of the dynamics of the stabilizing mechanism and can thus be omitted.

© 2020 The Authors. Published by Elsevier Ltd. This is an open access article under the CC BY license (<http://creativecommons.org/licenses/by/4.0/>).

## 1. Introduction

Assessing changes in human balance control, due to aging or pathologies such as Parkinson's disease and stroke, is important to provide for appropriate rehabilitation therapies which reduce the fall risk. Often, the ankle torque is used to assess unperturbed balance (Masani et al., 2013; Patel et al., 2011; Vette et al., 2010) or perturbed balance using perturbations such as platform translations (Afschrift et al., 2018; Hall et al., 1999; Hemami et al., 2006; Jones et al., 2012; Kim et al., 2009). Platform translations could also be combined with system identification techniques where the body sway and ankle torque are used to obtain the frequency response function (FRF), describing the dynamics of the stabilizing mechanism (STM) (Van Asseldonk et al., 2006;

Boonstra, 2014). However, in experimental settings, large, expensive and complex motion platforms are often used to perturb the body, which hampers clinical implementation.

A treadmill could be a simple alternative to apply support surface translations, which could be used in the clinic, but brings with it two main questions. The first question is whether the STM stiffness, i.e. the low frequency magnitudes of the frequency response function (Boonstra, 2014; Kearney et al., 1997; Lee et al., 2014; Schouten et al., 2008; Trevino and Lee, 2018), could correctly be estimated using a treadmill in combination with system identification methods. The STM stiffness is required to keep the body upright in a gravitational field, and consists of the passive muscle stiffness and active neural stiffness. No previous studies, however, validated the estimation of the STM stiffness using a treadmill in combination with system identification methods. The second question is what the effect of horizontal ground reaction forces is on estimation of the ankle torque and thereby on the STM dynamics. Although it is generally known that horizontal ground reaction

\* Corresponding author at: Biomechanical Engineering Department, Delft University of Technology, Delft, Mekelweg 2, 2628 CD, Netherlands.

E-mail address: [i.m.schut@tudelft.nl](mailto:i.m.schut@tudelft.nl) (I.M. Schut).

forces are substantially lower than vertical ground reaction forces, it is not clear what errors are made when the horizontal ground reaction forces are omitted in calculating the ankle torques and the stabilizing mechanism. The ankle torque is calculated by summing the vertical ground reaction forces multiplied by the centre of pressure (CoP) and the horizontal ground reaction forces multiplied by the height of the ankle joint (Fig. 1). However, measuring horizontal ground reaction forces with a treadmill requires a complex and expensive construction.

In this study we assessed human balance control with support surface translations and system identification using a treadmill. Firstly, we validated the STM stiffness estimation using an inverted pendulum, i.e. a single inverted pendulum with fixed STM stiffness. The fixed STM stiffness was measured by applying several forces and measuring the deviation, where the slope indicates the spring stiffness. The derived STM stiffness was compared with a dynamic system identification approach. Secondly, we investigated the effect of horizontal ground reaction forces on the estimation of the ankle torque and STM dynamics.

## 2. Methods

### 2.1. Subjects

To validate the STM stiffness estimation, an inverted pendulum (length 1.00 m) was used, consisting of a stick mounted on a brick via a piece of rubber. To investigate the effect of horizontal forces on the ankle torque and STM dynamics, twelve healthy volunteers participated (six women, median age 26, range 24–65 years, length  $1.73 \pm 0.09$  m, weight  $73.67 \pm 14.19$  kg). The study was approved by the local Human Research Ethics Committee and performed according to the principles of the Declaration of Helsinki.

### 2.2. Apparatus and recording

Balance was perturbed using a dual-belt treadmill (GRAIL, Motekforce Link, Amsterdam, The Netherlands) by anterior-

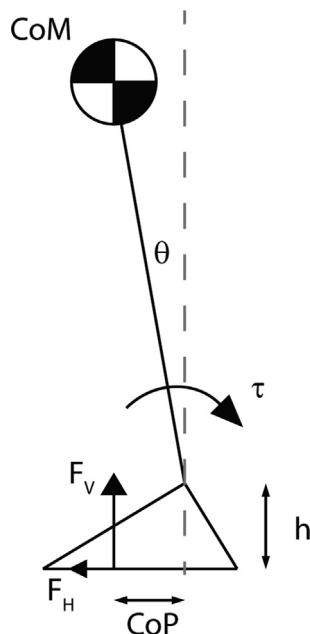


**Fig. 1.** Free body diagram of an inverted pendulum. The joint torque ( $\tau$ ) is calculated by summing the vertical ground reaction forces ( $F_v$ ) multiplied by the centre of pressure (CoP) and the horizontal ground reaction forces ( $F_h$ ) multiplied by the height of the joint ( $h$ ).

posterior translations of both belts synchronously. A 6-DOF force plate under each belt recorded ground reaction forces (1 kHz).

Twelve cameras captured (Bonita, Vicon motion Systems, United Kingdom) marker positions (100 Hz). Seven retroreflective markers were attached on the inverted pendulum: three on the stick, one on the rubber and three on the brick. Eight markers were attached to the participants' acromioclavicular joints, major trochanters, lateral epicondyles, and lateral malleoli of both left and right side. Two markers were placed on both belts.

### 2.3. Perturbation signal

The perturbation signal was a multisine signal with a period of 20 s, exciting 18 frequencies in the range of 0.05–5 Hz at a logarithmic frequency grid. The signal had a flat velocity spectrum, except for the magnitude of the first frequency (0.05 Hz), which was 1/3 of the magnitude of the second frequency (0.15 Hz), to prevent dominance of the lowest frequency in the translations. The signal was repeated 6.5 times resulting in trials of 130 s.

### 2.4. Procedures

To validate the estimation of the STM stiffness, the inverted pendulum's STM stiffness estimated using system identification was compared with the STM stiffness estimated using a regression method.

In the regression method, the STM stiffness was measured by placing the inverted pendulum horizontal on a table allowing the stick to rotate freely without gravity interacting. Forces were applied perpendicularly on the most distal side of the stick and measured using a spring scale (Salter, Super Samson, range 0–1 kg), such that the stick was gradually loaded and unloaded 5 times over a displacement range of  $-0.35$  to  $0.35$  m in steps of  $0.05$  m, thereby compensating hysteresis.

In the system identification method, the inverted pendulum stood on the left belt such that the stick could pivot around the rubber in anterior-posterior direction. A static trial of 5 s was recorded to obtain the distance between the centre of mass (CoM) and the joint, i.e. the distance between the stick centre and pivot point. Four perturbed trials were recorded with perturbation amplitude of  $0.08$  m peak-to-peak (ptp).

To study the effect of horizontal ground reaction forces on the estimation of the ankle torque and STM dynamics, participants stood on the treadmill as normal as possible without moving the feet and with arms crossed in front of the chest. First, a 5 s static trial was performed to obtain the participants weight and distance between the CoM and ankle joint. Four trials with perturbation amplitude of  $0.08$  m ptp were recorded. To study whether the relative effect of horizontal ground reaction forces is independent of perturbation amplitude, six additional trials with amplitudes of  $0.02$ ,  $0.05$ ,  $0.11$ ,  $0.14$ ,  $0.17$  and  $0.20$  m ptp were recorded. All perturbed trials were presented in random order.

### 2.5. Data pre-processing

Data were processed in Matlab (MathWorks, USA). Force plate data were resampled to 100 Hz to match the sample frequency of the marker data. For visualization, force plate data and marker data were zero-phase filtered by applying a 2nd order 5 Hz low pass Butterworth filter in forward and time-reversed direction.

The static trials were used to obtain the mass and distance between the CoM and the (ankle) joint, according to Winter (2009).

For each perturbed trial, the first 8 and last 2 s were discarded to remove transient effects, leaving 120 s, and subsequently cut in 6 segments of 20 s, i.e. the period length of the multisine. The segments of the four trials with amplitude  $0.08$  m ptp were combined,

resulting in 24 segments. For the analysis regarding the influence of perturbation amplitude, only the first trial with amplitude 0.08 m ptp was used.

Belt and subject marker positions were used to respectively obtain the perturbation torque according to (Van Asseldonk et al., 2006) and the body sway (BS), which was defined as the angle of the CoM with respect to vertical, using the anterior-posterior CoM position, and the distance between the CoM and the (ankle) joint.

For the CoP calculations of the validation measurements, vertical ground reaction forces were corrected for the force due to the mass of the brick, since the mass of the brick is large compared to the mass of the CoM. The CoP on each belt with respect to the joint was corrected for CoP displacements due to the mass of the brick according to

$$CoP = CoP_r - \frac{m_b \cdot \ddot{x}_{ss} \cdot 0.5z}{m_b \cdot 9.81} \quad (1)$$

with  $CoP_r$  the CoP with respect to the joint, i.e. the CoP derived from the force plates minus the joint marker position,  $m_b$  the mass of the brick and  $z$  the height of the brick, i.e.  $0.5z$  represents the height of the brick's CoM. For the human experiments, the CoP was calculated with respect to the joint.

For the validation, the joint torque was calculated with inverse dynamics (Van der Kooij et al., 2005; Koopman et al., 1995) according to

$$T = -F_V CoP - F_H h \quad (2)$$

With  $F_H$  and  $F_V$  the horizontal and corrected vertical ground reaction forces, respectively. To investigate the effect of horizontal ground reaction forces the participants' joint torques of both feet were calculated by 1) including  $F_H$  which is stated by Eqs. (2) and 2) neglecting  $F_H$  which results in Eq. (3)

$$T_{NH} = -F_V CoP \quad (3)$$

The ankle torque was obtained by adding the joint torques of both feet.

## 2.6. Data analysis

For the validation, the regression method was used to calculate the applied joint torque by multiplying the measured force with the length of the stick. The angular displacement was obtained from the stick displacements using goniometry. The slope of a fitted linear line represented the rotational stiffness, i.e. the STM stiffness.

The STM stiffness calculated with the regression method was compared with the stiffness calculated using the system identification method. The body sway and joint torque were transformed to the frequency domain using the fast Fourier transform resulting in  $T(f)$  and  $BS(f)$ , which were averaged and used to calculate the FRF, describing the STM dynamics in terms of a magnitude and phase, according to (Van der Kooij and De Vlugt, 2007; Schut et al., 2019)

$$FRF(f) = -\overline{T(f)} / \overline{BS(f)} \quad (4)$$

The bars indicate averaging over the segments. STM stiffness of the inverted pendulum was calculated by averaging the second and third excited frequencies (0.15–0.35 Hz), as the coherence and signal-to-noise ratio of the first excited frequency were low (see results).

Coherence was calculated according to

$$COH(f) = \frac{|\overline{S_{uy}(f)}|^2}{\overline{S_{uu}(f)} \overline{S_{yy}(f)}} \quad (5)$$

With  $S_{uu}$  and  $S_{yy}$  representing the spectral densities of body sway and joint torque respectively and  $S_{uy}$  the cross spectral density from body sway to torque.

The variance accounted for (VAF) was calculated according to

$$VAF = \left( 1 - \frac{\overline{\text{var}(T(t) - T_{NH}(t))}}{\overline{\text{var}(T(t))}} \right) \cdot 100\% \quad (6)$$

The bars indicate averaging over the segments to reduce measurement noise. A VAF of 100% means that 100% of the ankle torque ( $T$ ) is explained by  $T_{NH}$ , i.e. the horizontal ground reaction forces do not contribute.

Two FRFs and their coherences were calculated by (1) including  $F_H$  (FRF), and (2) neglecting  $F_H$  (FRF<sub>NH</sub>) according to the method described above. For each FRF the STM stiffness was calculated by averaging the first three excited frequencies. In addition, the magnitudes were averaged over a low (0.05–0.95 Hz), mid (1.00–2.35 Hz) and high (2.40–4.95 Hz) frequency group, in which the stiffness, damping and inertia respectively dominate the magnitude. Relative errors (RE) were calculated for the STM stiffness and frequency groups by subtracting the FRF<sub>H</sub> magnitude from the FRF<sub>NH</sub> magnitude and dividing by the FRF<sub>NH</sub> magnitude.

## 3. Results

### 3.1. Validation

Linear regression on the data resulted in

$$T = 4.78\theta + 0.03 \quad (7)$$

with  $\theta$  the angular rotation and 4.78 representing the STM stiffness in Nm/rad, with a standard error of ( $\pm 0.06$ ) (Fig. 2).

The time series of the belt position, body sway and torque were as expected (Fig. 3). The STM stiffness of  $5.08 \pm 0.22$  Nm/rad, estimated using system identification (Fig. 4), was within 6% of the joint stiffness calculated with the regression method (4.78 Nm/rad).

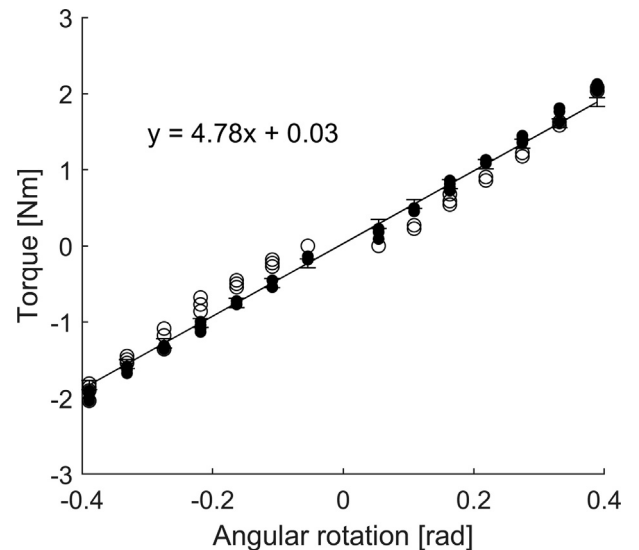


**Fig. 2.** Torque versus angular rotation. Black dots represent loading, white dots represent unloading. The black line represents the linear fit with function  $y = 4.78x + 0.03$ . The hysteresis can be seen by the difference in required torque for loading (black dots) and unloading (white dots).

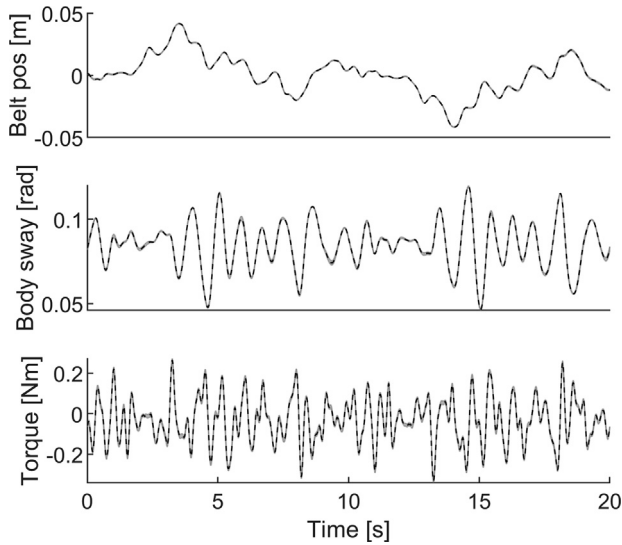


**Fig. 3.** Mean (black) of the inverted pendulums belt position (top), body sway (middle) and torque (bottom). The grey areas represent the standard deviation, which is small.

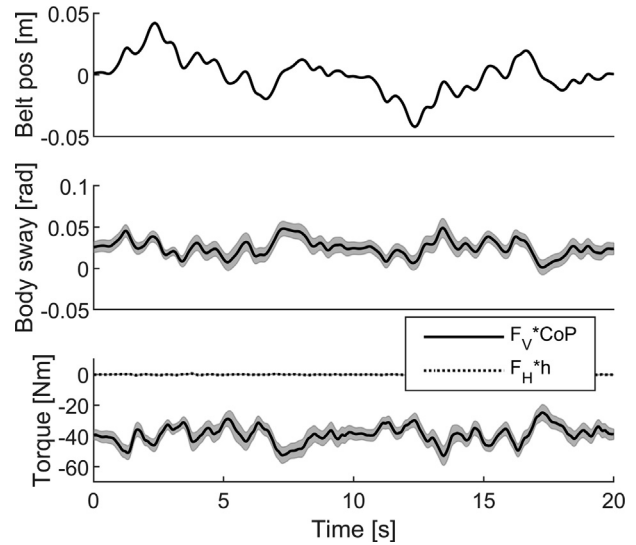


**Fig. 5.** Mean belt position (top), body sway (middle) and torque (bottom) calculated by neglecting horizontal ground reaction forces (solid) and neglecting vertical ground reaction forces (dotted) of one typical participant, averaged over 24 segments. The grey areas represent the standard deviation.

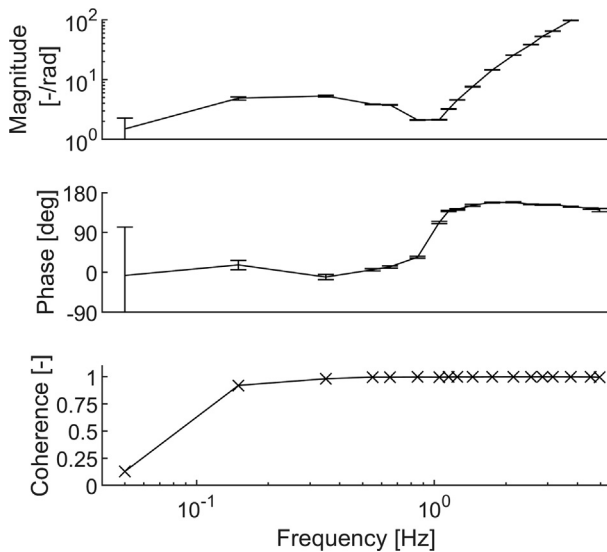


**Fig. 4.** Mean magnitude normalized for gravitational stiffness (top), phase (middle) and coherence (bottom) of the frequency response function of the inverted pendulum, averaged over the 24 segments. The error bars indicate the standard deviation. Crosses indicate the excited frequencies.

### 3.2. Effect of horizontal ground reaction forces

All participants showed a low contribution of  $F_H$  and  $h$  to the calculation of the ankle torque compared to the contribution of  $F_V$  and  $CoP$  (Fig. 5). This resulted in a high VAF of  $99.9 \pm 0.2\%$  averaged over participants. Body sway increased with perturbation amplitude and resulted in larger  $F_H$  and  $CoP$  (not shown). The relative contribution of  $F_H$  to the ankle torque was constant over amplitude, resulting in VAFs between  $99.8 \pm 0.3\%$  and  $99.9 \pm 0.1\%$  (Table 1).

The FRF magnitudes, normalized for the gravitational stiffness (gravitational constant multiplied by mass and distance between  $CoM$  and ankle joint) and averaged over participants, were as expected, with high coherence for the low frequencies (Fig. 6). The low frequencies, representing the stiffness, had values around 1, indicating that the stiffness provided by the human was sufficient to compensate the pull of gravity. There was a small dip within the mid frequencies, representing the damping, and the

**Table 1**

Mean and standard deviation of the body sway and VAFs for all conditions, averaged over participants. The SD represents the standard deviation.

Amplitude (m ptp)	Body sway ( $^\circ$ ptp)		VAF (%)	
	Mean	SD	Mean	SD
0.02	1.1	0.3	99.9	0.1
0.05	2.1	0.4	99.8	0.2
0.08	3.1	0.5	99.8	0.2
0.11	3.8	0.4	99.8	0.2
0.14	4.7	0.6	99.8	0.3
0.17	5.4	0.6	99.8	0.2
0.20	6.4	0.7	99.8	0.2

magnitudes increase at the high frequencies, representing the inertia. The  $FRF_{NH}$  magnitude is almost identical to the normalized  $FRF_{NH}$  magnitude, especially for the lower frequencies. There is no difference in STD stiffness between the STD stiffness of  $FRF_{NH}$  and  $FRF$  (error relative to  $FRF_{NH}$  (RE) =  $-0.38\%$ ) (Table 2). The RE is  $-0.68$ ,  $0.66$  and  $-14.7\%$  for the low, mid and high frequencies respectively. The phases of  $FRF_{NH}$  and  $FRF$  are similar (Fig. 6). REs were similar over different perturbation amplitudes (not shown).

## 4. Discussion

### 4.1. Validation

The STM stiffness of the inverted pendulum estimated with the regression method was similar to the STM stiffness estimated with the system identification method (difference 6%). This indicates that the STM stiffness could be estimated using the system identification method in combination with support surface translations.

### 4.2. Effect of horizontal ground reaction forces

The effect of horizontal ground reaction forces on the ankle torque was negligible as more than 99.8% of the ankle torque was explained by the vertical ground reaction forces and  $CoP$ . This effect is independent of the perturbation amplitude as long as the induced body sway stays within a range of  $1.1$ – $6.4^\circ$  ptp, a com-

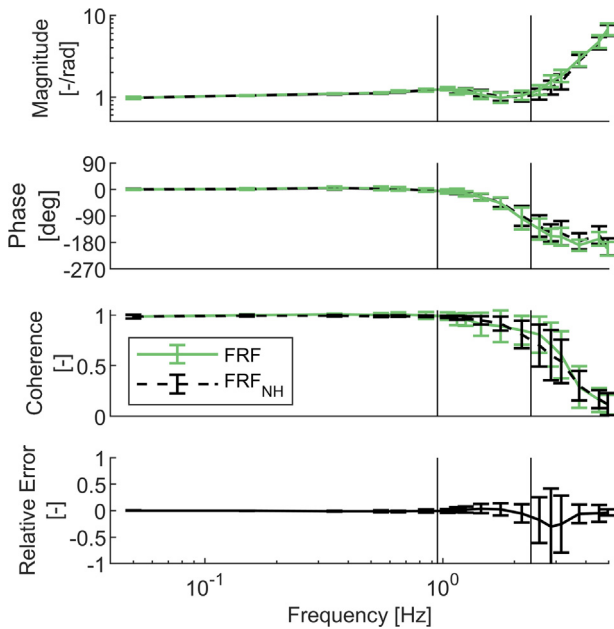


**Fig. 6.** Mean normalized magnitude (top), phase (2nd row), coherence (3rd row) and relative error (bottom) of the frequency response function, calculated by including horizontal ground reaction forces (black) and by neglecting horizontal ground reaction forces (green), averaged over participants. The error bars indicate the standard deviation.

**Table 2**

Relative errors (RE) expressed as percentage, averaged over participants for the stiffness [0.05–0.35 Hz], low frequencies [0.05–0.95 Hz], mid frequencies [1.00–2.35 Hz] and high frequencies [2.40–4.95 Hz]. The SD represents the standard deviation.

	RE [%]	SD
Stiffness	−0.38	0.35
Low freqs	−0.68	1.16
Mid freqs	0.66	7.55
High freqs	−14.7	25.5

mon range in literature (Van Asseldonk et al., 2006; Boonstra, 2014; Jilk et al., 2014; Ko et al., 2013; Pasma et al., 2012; Schieppati et al., 2002). The effect of horizontal ground reaction forces on the FRF of the STM dynamics were small ( $|RE| < 15\%$ ), especially for the STM stiffness ( $|RE| < 0.5\%$ ), and the low and mid frequencies ( $|RE| < 1\%$ ).

To conclude, the STM stiffness of an inverted pendulum can be estimated using support surface translations in combination with system identification. Secondly, within the induced body sway angles, the horizontal ground reaction forces play a minor role in human balance and can be omitted to calculate the ankle torque, thereby still resulting in a reliable estimation of the STM stiffness and dynamics. This allows for the use of less complex treadmills that only measure vertical ground reaction forces and the centre of pressure.

### Acknowledgements

This work is part of the research programme Innovative Medical Devices Initiative (IMDI) NeuroControl with project number

104003014, which is (partly) financed by the Netherlands Organisation for Health Research and Development (ZonMw).

### References

- Afschrift, M., De Groot, F., Verschueren, S., Jonkers, I., 2018. Increased sensory noise and not muscle weakness explains changes in non-stepping postural responses following stance perturbations in healthy elderly. *Gait Posture* 59, 122–127.
- Boonstra, T.A., Van Vugt, J.P.P., Van der Kooij, H., Bloem, B.R., 2014a. Balance asymmetry in Parkinson's disease and its contribution to freezing of gait. *PLOS One* 9.
- Boonstra, T.A., Schouten, A.C., Van Vugt, P.P., Bloem, B.R., Van der Kooij, H., 2014b. Parkinson's disease patients compensate for balance control asymmetry. *J. Neurophysiol.* 112, 3227–3239.
- Hall, C.D., Woollacott, M.H., Jensen, J.L., 1999. Age-related changes in rate and magnitude of ankle torque development: Implications for balance control. *J. Gerontol.* 54a (10), M507–M513.
- Hemami, H., Barin, K., Pai, Y., 2006. Quantitative analysis of the ankle strategy under translational platform disturbance. *IEEE Trans. Neural Syst. Rehabil. Eng.* 14 (4), 470–480.
- Jilk, D.J., Safavynia, S.A., Ting, L.H., 2014. Contribution of vision to postural behaviors during continuous support-surface translations. *Exp. Brain Res.* 232, 169–180.
- Jones, S.L., Hitt, J.R., DeSarno, M.J., Henry, S.M., 2012. Individuals with non-specific low back pain in an active episode demonstrate temporally altered torque responses and direction-specific enhanced muscle activity following unexpected balance perturbations. *Exp. Brain Res.* 221, 413–426.
- Kearney, R.E., Stein, R.B., Parameswaran, L., 1997. Identification of intrinsic and reflex contributions to human ankle stiffness dynamics. *IEEE Trans. Biomed. Eng.* 44 (6), 493–504.
- Kim, S., Horak, F.B., Carlson-Kuhta, P., Park, S., 2009. Postural feedback scaling deficits in Parkinson's disease. *J. Neurophysiol.* 102, 2910–2920.
- Ko, J., Challis, J.H., Newell, K.M., 2013. Postural coordination patterns as a function of rhythmical dynamics of the surface of support. *Exp. Brain Res.* 226, 183–191.
- Koopman, B., Grootenboer, H.J., De Jongh, H.J., 1995. An inverse dynamics model for the analysis, reconstruction and prediction of bipedal walking. *J. Biomech.* 28, 1369–1376.
- Lee, H., Krebs, H.I., Hogan, N., 2014. Multivariable dynamic ankle mechanical impedance with active muscles. *IEEE Trans. Neural Syst. Rehabil. Eng.* 22, 971–981.
- Masani, K., Sayenko, D.G., Vette, A.H., 2013. What triggers the continuous muscle activity during upright standing? *Gait Posture* 37, 72–77.
- Pasma, J.H., Boonstra, T.A., Campfens, S.F., Schouten, A.C., Van der Kooij, H., 2012. Sensory reweighting of proprioceptive information of the left and right leg during human balance control. *J. Neurophysiol.* 108, 1138–1148.
- Patel, M., Fransson, P.A., Johansson, R., Magnusson, M., 2011. Foam posturography: standing on foam is not equivalent to standing with decreased rapidly adapting mechanoreceptive sensation. *Exp. Brain Res.* 208, 519–527.
- Schieppati, M., Giordano, A., Nardone, A., 2002. Variability in a dynamic postural task attests ample flexibility in balance control mechanisms. *Exp. Brain Res.* 144, 200–210.
- Schouten, A.C., Mugge, W., Van der Helm, F.C.T., 2008. NMClab, a model to assess the contributions of muscle visco-elasticity and afferent feedback to joint dynamics. *J. Biomech.* 41, 1659–1667.
- Schut, I.M., Pasma, J.H., De Van der Veij Mestdagh, J.C., Kooij, H., Schouten, A.C., 2019. Effect of amplitude and number of repetitions of the perturbation on system identification of human balance control during stance. *IEEE Trans. Neural Syst. Rehabil. Eng.* 27 (12), 1–8.
- Trevino, J., Lee, H., 2018. Sex difference in 2-DOF human ankle stiffness in relaxed and contracted muscles. *Ann. Biomed. Eng.* 46, 2048–2056.
- Van Asseldonk, E.H.F., Buurke, J.H., Bloem, B.R., Renzenbrink, G.J., Nene, A.V., Van der Helm, F.C.T., Van der Kooij, H., 2006. Disentangling the contribution of the paretic and non-paretic ankle to balance control in stroke patients. *Exp. Neurol.* 201, 441–451.
- Van der Kooij, H., De Vlugt, E., 2007. Postural responses evoked by platform perturbations are dominated by continuous feedback. *J. Neurophysiol.* 98, 730–743.
- Van der Kooij, H., Van der Van Asseldonk, E.H.F., Helm, F.C.T., 2005. Comparison of different methods to identify and quantify balance control. *J. Neurosci. Methods* 145, 175–203.
- Vette, A.H., Masani, K., Nakazawa, K., Popovic, M.R., 2010. Neural-Mechanical feedback control scheme generates physiological ankle torque fluctuation during quiet stance. *IEEE Trans. Neural Syst. Rehabil. Eng.* 18 (1), 86–95.
- Winter, 2009. *Biomechanics and motor control of human movement*. John Wiley and Sons Inc, New Jersey, pp. 82–106.